Available online at www.sciencedirect.com
SCIENCE DIRECT®
Advances in Space Research 37 (2006) 1031–1037
ADVANCES IN SPACE RESEARCH (a COSPAR publication)
www.elsevier.com/locate/asr

Numerical models of the E-region ionosphere

Stanley C. Solomon *

National Center for Atmospheric Research, High Altitude Observatory, 1850 Table Mesa Drive, P.O. Box 3000, Boulder, CO 80307, United States

Received 23 November 2004; received in revised form 30 July 2005; accepted 13 September 2005

Abstract

Although the ambient E-region of the ionosphere has been fairly well characterized in the non-auroral regions with respect to density, ion composition, and variability, it is not as well understood as might be expected from a theoretical point of view. This is due primarily to uncertainties in the solar irradiance that produces E-region ionization (mainly the H Lyman-β line and the soft X-ray region), and to the variability of odd-nitrogen species that control ion composition. Recent measurements from the SNOE, TIMED, and SORCE satellites have greatly improved our quantitative understanding of both solar spectral irradiance and lower thermosphere nitric oxide, which in turn improves our ability to accurately model the E-region. The new measurements indicate higher solar soft X-ray irradiance but lower flux in the H Lyman-β line than earlier estimates by Hinteregger et al. [Hinteregger, H.E., Fukui, K., Gilson, B.R., Observational, reference, and model data on soalr EUV, from measurements on AE–E. Geophys. Res. Lett. 8 (1981) 1147] based on measurements from Atmosphere Explorer and from rocket flights. However, preliminary results from the Solar EUV Experiment (SEE) on the TIMED satellite are in better agreement with the EUVAC model [Richards, P.G., Fenenelly, J.A., Torr, D.G., EUVAC: a solar EUV flux model for aeronomic calculations. J. Geophys. Res. 99 (1994) 8981–8992]. This raises the question of whether either of these representations of the solar spectrum can adequately represent E-region electron density and variation. Model simulations of the E-region using these two solar model inputs are compared to the International Reference Ionosphere (IRI) empirical model, which has been validated using measurements from the Boulder ionosonde. Calculations using the Hinteregger et al. solar inputs significantly underestimate the peak electron densities at all levels of activity, while using EUVAC solar inputs produces better agreement but slightly more variability than the empirical representations. As improved estimates of variability from TIMED/SEE over a complete solar cycle become available, these remaining discrepancies may be resolved.

Keywords: Ionosphere; Solar EUV irradiance; Photochemistry

1. Introduction

The E-region of the ionosphere, the region between ~100 and ~140 km altitude, is characterized by a modest peak in the electron density profile located near 105–110 km. This peak is due to photoionization of O_2 by the solar H Lyman-β line at 102.6 nm and photoionization of all atmospheric gasses (but mostly N_2) by solar soft X-rays in the ~1–20 nm range. At slightly higher altitudes, the CIII line at 97.7 nm and other solar emissions in the 90–100 nm region play a significant role; near twilight, ionization of nitric oxide by H Lyman-α at 121.6 nm becomes important; in the polar regions, auroral particle fluxes also cause E-region ionization; at night, metallic ion layers can be prominent. Nevertheless, the non-auroral daytime peak E-region electron density N_mE is almost entirely a function of H Lyman-β, soft X-rays, and the atmospheric composition and temperature.

For some decades, the canonical view of the E-region was that solar H Lyman-β was the principal source. The reference spectrum and scaling factors obtained by Hinteregger et al. (1981) (HFG) from the Atmosphere Explorer (AE) program and from rocket measurements supported relatively high Lyman-β flux and variability of as much as a factor of 3 over the solar cycle, while yielding relatively small fluxes shortward of ~20 nm. However, although this

* Tel.: +1 303 497 2179.
E-mail address: stans@ucar.edu.

0273-1177/$30
doi:10.1016/j.asr.2005.09.040

reference spectrum has been considered an acceptable standard in the extreme ultraviolet (EUV), recent findings have shown that its validity in the soft X-ray region is questionable. The problem dates back to comparisons with AE photoelectron measurements by Richards and Torr (1984), and was reviewed by Solomon (1991). Broad-band ionization cell and photodiode measurements from suborbital vehicles (e.g., Feng et al., 1989; Ogawa et al., 1990; Bailey et al., 1999) indicated that the HFG model underestimates solar soft X-rays. Work by Buonsanto et al. (1992, 1995) found a significant shortfall in models of the E and F_1 region ionosphere between 100 and 200 km, when compared to incoherent scatter radar and ionosonde measurements (cf., Titheridge, 2000; Kazil et al., 2003). The EUVAC model of Richards et al. (1994), based on a reanalysis of some of the same data sets used by Hinteregger et al., adjusted the soft X-rays upward by a factor of ~2–3, depending on spectral region. Finally, measurements by the solar X-ray photometer on the SNOE satellite found considerably higher soft X-ray fluxes than the HFG model, a factor of ~4 at all levels of solar activity (Bailey et al., 2000). Solomon et al. (2001) used the SNOE measurements in new model calculations of photoelectron fluxes and ion densities, and obtained much better agreement with the AE photoelectron measurements and the Buonsanto et al. (1992, 1995) electron density measurements. The relatively high levels of nitric oxide measured by SNOE also lends weight to the idea that solar soft X-rays had previously been greatly underestimated.

2. Preliminary measurements by the TIMED solar EUV experiment

2.1. Measurement description

The TIMED mission was launched on 7 December 2001 and the solar EUV experiment (SEE) began making solar measurements in January 2002. SEE consists of two instruments, a spectrograph that covers the range 27–175 nm at a resolution of 0.4 nm, and a group of silicon photodiodes that measure soft X-rays in bands of ~5–10 nm width. The instruments and initial results are described by Woods et al. (2005). In Fig. 1, sample spectra from TIMED/SEE are shown, including one at high solar activity on the 8 February 2002, the day of the initial rocket calibration, and another on 22 March 2003 at low-to-moderate solar activity. These spectra are level 3 data (daily average spectra in 1-nm bins, flares excluded) from version 7.0 of the SEE data processing.

Because the spectral irradiance shortward of 27 nm is estimated using broad-band photodiodes, its wavelength dependence and, to a lesser extent, its overall magnitude, is dependent on the model assumptions used to construct the 1-nm spectrum. Since March 2003, the soft X-ray spectra in the SEE level 3 data are actually calculated using similar photodiodes on the SORCE spacecraft (Woods et al., 2000). Longward of 27 nm, the spectrograph

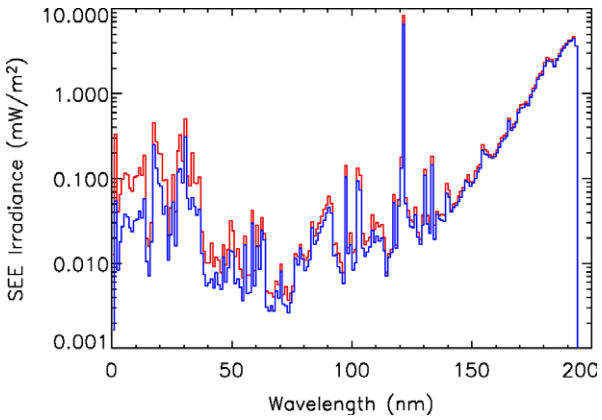

Fig. 1. Examples of daily average solar X-ray/EUV/FUV spectrum from the Thermosphere–Ionosphere–Mesosphere Energetics and Dynames (TIMED) Solar EUV Experiment (SEE). Red line: solar irradiance on 8 February 2002 at high solar activity. Blue line: solar irradiance on 22 March 2003 at low-to-moderate solar activity.

measurements have been calibrated pre-flight using a synchrotron source and in-flight by suborbital measurements, and are certainly the most accurate and precise measurements obtained to date in the EUV.

2.2. Soft X-ray and H Lyman-β measurements and comparison to models

Preliminary results from TIMED/SEE have found that the magnitude and variability of the solar EUV and soft X-ray spectrum is in rough agreement with the EUVAC model through most of its spectral range. Since the soft X-ray intensity remains controversial, and since SEE has limited ability to infer its spectral distribution, an initial comparison is shown in Fig. 2 using a wide integration from 0 to 20 nm. The EUVAC model only extends to 5 nm, so from 1.8 to 5 nm the HFG spectrum multiplied by a factor of 3 is included. Shortward of 1.8 nm (in non-flare conditions) the contribution to the total flux is insignificant. The comparison with EUVAC and HFG as shown demonstrates that TIMED/SEE better supports the reanalysis by Richards et al. (1994). These preliminary results are somewhat smaller than the SNOE results, but still considerably larger fluxes than the HFG model.

Also shown in Fig. 2 is a comparison of TIMED/SEE measurements of the solar H Lyman-β line with the EUVAC and HFG models. In this case, HFG greatly overestimates the magnitude and variability of the line flux, but EUVAC agrees quite well. For this preliminary result, the line flux was estimated by taking the average of the daily line-fit measurements and the 102–103 nm bin in the level 3 spectrum. The line-fit slightly underestimates the actual H Lyman-β flux, while the 102–103 nm bin slightly overestimates the actual flux, due to the proximity of bright oxygen lines in the 103–104 nm range [F.G. Eparvier, personal communication, 2004]. This introduces a small additional uncertainty, of the order of 20%, in addition to the

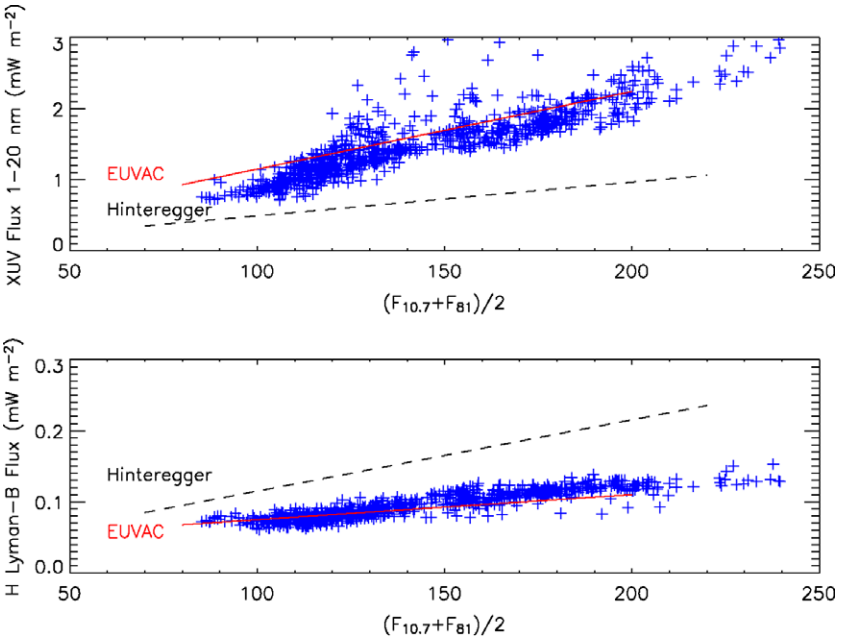

Fig. 2. Comparison of preliminary TIMED/SEE solar irradiance between 0 and 20 nm and at H Lyman-β (102.6 nm) to the HFG (Hinteregger et al., 1981) and EUVAC (Richards et al., 1994) models. Blue plusses: measurements. Solid red line: EUVAC model. Dashed black line: HFG model.

~10% calibration uncertainty. However, this is far less than the disagreement with HFG.

3. The international reference ionosphere E-region model

3.1. Model description

The International Reference Ionosphere (IRI) (Bilitza, 2001) contains a simple model for the daytime E-region peak electron density N_mE with a nearly constant peak altitude H_mE at ~107 km. This latter assumption is adequate for low ($< \lesssim 60°$) solar zenith angles, but is clearly inadequate at near-twilight solar zenith angles, where H_mE increases according to both observation and theory. However, for our purpose of comparing peak electron densities with solar fluxes, the assumption of a fixed H_mE is unimportant. There is an option within the IRI model to use the E-region model of Friedrich and Torkar (2001), which does allow H_mE variation. However, for this study, the standard "Edinburgh method" N_mE model (Kouris and Muggleton, 1973a,b; Trost, 1979) is employed. This simple parameterization is based on the idea that the basic factors controlling the daytime E-region are the level of solar activity, the solar zenith angle, geographic latitude, and a seasonal effect, which is captured by the solar zenith angle at noon. An example of the global distribution of N_mE predicted by IRI is shown in Fig. 3. The component of the parameterization defining solar activity effects on the E-region is:

$$A = [1 + 0.0094(\langle F_{10.7}\rangle - 66)]^{1/2},$$

where $\langle F_{10.7}\rangle$ is the running annual mean of the solar 10.7 cm radio flux index (ranging from ~70 to ~210). Thus, the Edinburgh parameterization predicts a solar cycle variation in N_mE of about a factor of 1.5.

3.2. Comparison to selected N_mE measurements

Since this model is based on ionosonde measurements prior to the mid-1970s, it is instructive to validate its conclusions against a long-term record of N_mE at particular ionosonde locations. For an initial study, 20 years of data from the ionosonde at Boulder, Colorado were obtained from the National Geophysical Data Center (http://www.ngdc.noaa.gov) covering the time period 1980–2000. These data were used because they form a reasonably complete and continuous record over several solar cycles. Results of this comparison are shown in Fig. 4. Noon data are employed to eliminate the diurnal effect, and then data from the vernal equinoxes are selected to also eliminate the seasonal effect. A linear fit to the model versus the data shows excellent agreement with respect to both slope and intercept, demonstrating that this simple and venerable parameterization has adequately captured solar cycle variation of N_mE, at least at this particular location and for this particular instrument.

4. Numerical modeling of the E-region

4.1. Model description

Ionization rates, photoelectron fluxes, and ion/electron densities are calculated using the GLOW model (Solomon et al., 1988; **?**; Bailey et al., 2002). The neutral atmosphere is specified by the MSIS-86 semi-empirical model (Hedin, 1987). For solar input, the HFG (Hinteregger

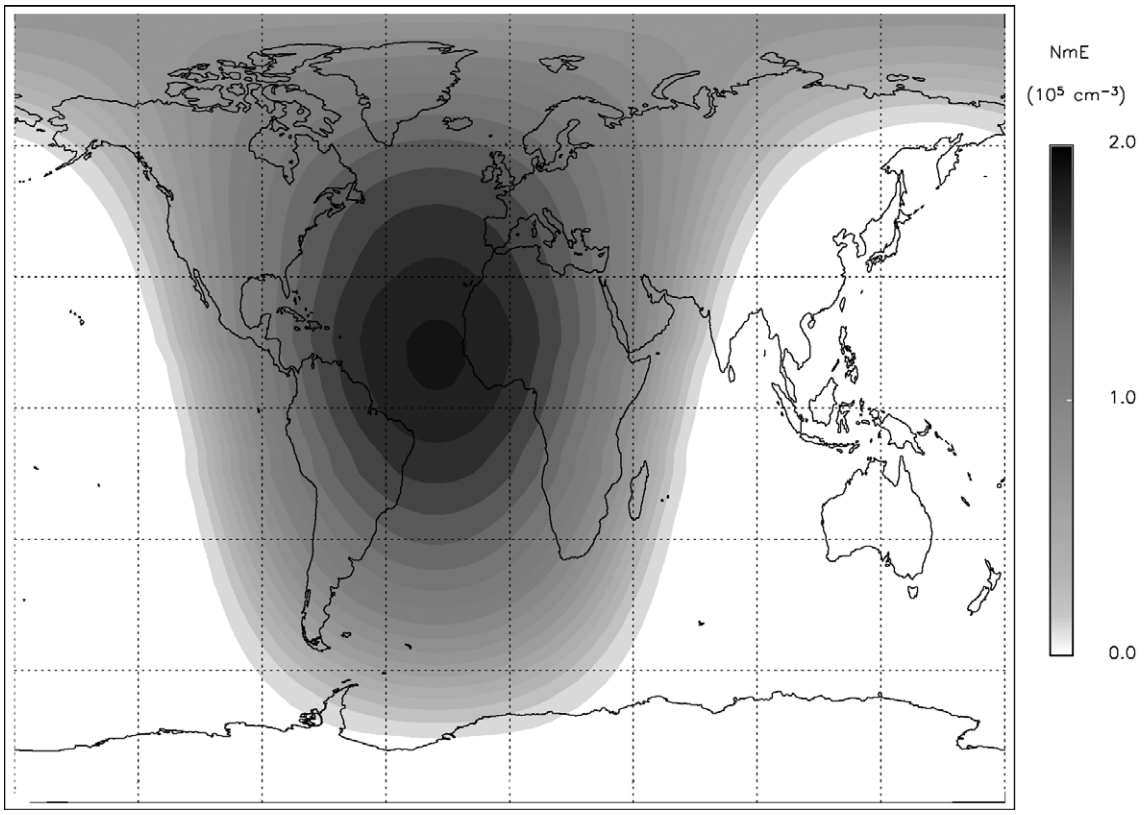

Fig. 3. Peak E-region electron density from the IRI model for 24 July 2004 at 14:00 UTC for $\langle F_{10.7}\rangle = 150$.

et al., 1981) or EUVAC (Richards et al., 1994) models are used.

The lifetimes of ions and electrons in the 100–200 km region are on the order of a minute, so transport of the ambient ionosphere is nearly negligible. Thus, a photochemical equilibrium model is valid. There are some exceptions to this: rapid vertical motions or long-lived metallic ions can make transport processes significant. These processes are not included here, but photoelectron transport is included at all model altitudes. K-shell ionization and consequent Auger electrons are included in the model, to fully account for ionization caused by solar photons shortward of 3 nm.

The ion chemistry of the E-region is much simpler than other ionospheric regions because the electron density loss rate is entirely controlled by dissociative recombination of the main molecular ion species, NO^+ and O_2^+. Ionization of N_2 by soft X-rays and photoelectrons is rapidly converted to O_2 by the charge exchange reaction $N_2^+ + O_2 \rightarrow N_2 + O_2^+$, and the balance between O_2^+ and NO^+ is controlled by the nitric oxide density because of the reaction $O_2^+ + NO \rightarrow O_2 + NO^+$. Reactions involving atomic oxygen and atomic nitrogen are included in the model but below ~120 km they have very little effect on electron density. Because NO^+ recombines more rapidly than O_2^+, the NO density does have a small effect, so parameterized NO measurements from SNOE are used to provide a model profile.

Fig. 5 shows examples of calculated E-region electron density profiles. The EUVAC inputs yield higher electron density at all altitudes, and a slightly higher H_mE, due to the increased ionization by soft X-rays. Also, it is noteworthy that using EUVAC produces a much less pronounced peak, particularly at solar minimum, and scarcely any "valley" at all.

4.2. Comparison to IRI

Results of the comparison between numerical and empirical models for N_mE are shown in Fig. 6. To maintain compatibility with the analysis shown in Section 3.2, noon vernal equinox conditions at Boulder were used, but for any constant solar time, latitude, and season, the conclusions would be similar. Both solar inputs to the GLOW model result in underestimates when compared to IRI, and both cases overestimate the solar cycle dependence (note that since this is a linear scale, similar slopes do not imply similar variability). However, the model with EUVAC inputs is much closer to the IRI parameterization than it is with HFG inputs, particularly at solar maximum.

Uncertainties in the model stem primarily from the solar EUV fluxes themselves, and are approximately spanned by the two model input examples shown in Fig. 6. There are additional numerical model uncertainties caused by dissociative recombination rate, electron temperature, and ion composition uncertainties, which are of the order of ~20% for N_mE (cf., Doe et al., 2005). The uncertainties in N_mE for IRI, when used in this statistical manner, are estimated from Fig. 4 to be ~10%. Therefore, the agreement

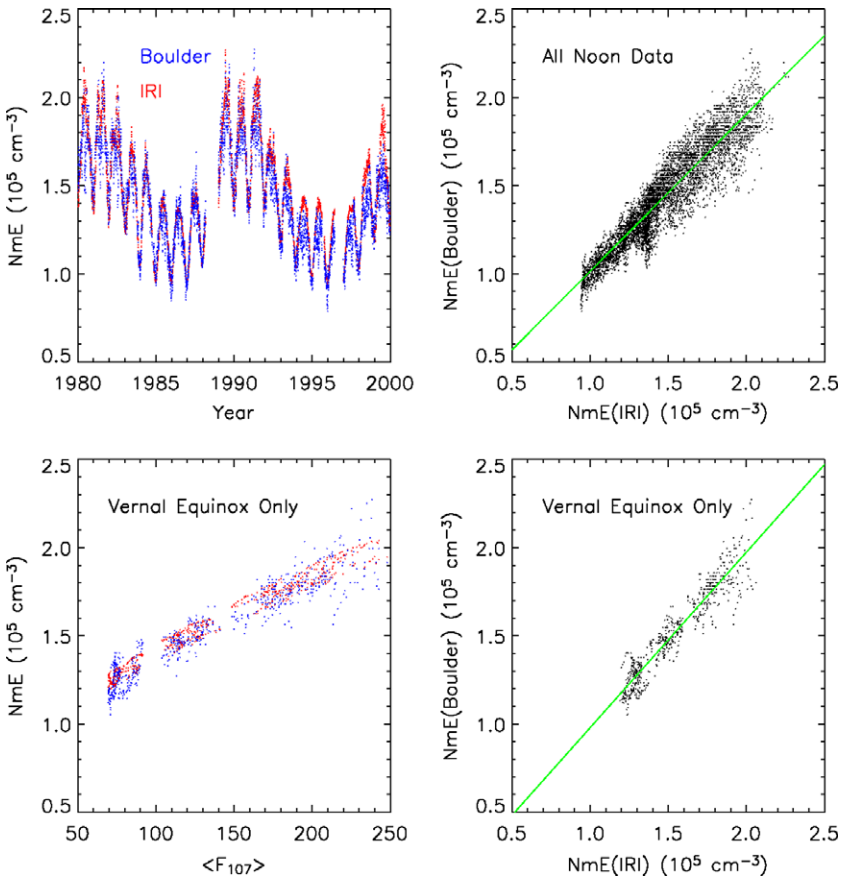

Fig. 4. Comparison of 20 years of Boulder ionosonde measurements of $N_m(E)$ with the IRI model. Upper left: time series of noon (±1 h) data (red dots) and model (red dots). Upper right: scatter comparison of data and model with linear fit. Lower left: noon data (blue dots) and model (red dots) within ±20 days of the vernal equinox as a function of $\langle F_{10.7} \rangle$. Lower right: scatter comparison of noon vernal equinox data with linear fit.

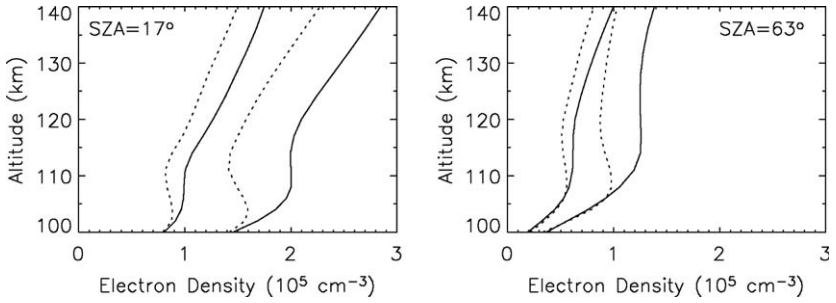

Fig. 5. Example E-region electron density profiles calculated using the GLOW model with different solar inputs. Left: calculation for latitude 40°, longitude −105°, at local noon at summer solstice (solar zenith angle 17°) for solar minimum ($F_{10.7} = 70$) and maximum ($F_{10.7} = 230$) conditions. Right: same for local noon conditions at winter solstice (solar zenith angle 63°). Dotted line: HFG solar input. Solid line: EUVAC solar input.

between the calculation using EUVAC and IRI is adequate at solar maximum but barely within expected limits at solar minimum. For the calculation using the Hinteregger model, the comparison is outside of the range of estimated uncertainties throughout the range of solar activity.

5. Discussion

If the TIMED/SEE results for solar H Lyman-β are correct, strong support is provided for the EUVAC parameterization and indirect support is provided for the increased soft X-ray fluxes. If H Lyman-β does not provide sufficient E-region ionization compared to observations, then something else must, and it is difficult to imagine what that could be if not soft X-rays. It is possible that the ion loss rates are overestimated, but since these are controlled entirely by dissociative recombination, and since these reaction rates have been well-established by multiple laboratory measurements, major revision is unlikely. E-region temperatures are not far from room temperature, where dissociative recombination rates are best known.

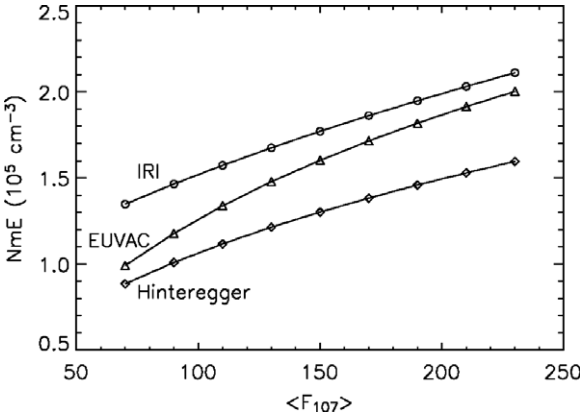

Fig. 6. Three models of E-region peak ion density $N_m(E)$ as a function of solar activity as represented by $\langle F_{10.7}\rangle$. Circles: IRI. Triangles: GLOW model with solar input from EUVAC. Diamonds: GLOW model with solar input from the HFG. Noon equinox conditions at Boulder, Colorado were used.

Both the EUVAC and HFG solar models still underestimate E-region ionization rates, particularly at solar minimum. Other models of the solar EUV and soft X-ray spectrum such as NRLEUV (Warren et al., 1998) and SOLAR2000 (Tobiska et al., 2000) have varying degrees of agreement with the new TIMED/SEE data, as discussed by Woods et al. (2005), but neither have soft X-ray fluxes high enough to remedy the problem given the lower H Lyman-β measurements from SEE. Titheridge (1997, 2000, 2003) similarly found that EUVAC would need to be scaled upward in order to obtain agreement with measured E-region ion densities. The NO densities (Titheridge, 1997) used in these studies were based on results from SME, which have now been superceded by the much higher values measured by SNOE and HALOE (e.g., Marsh et al., 2004). This compounds the problem due to the faster NO^+ recombination rate, but may improve model correspondence with the seasonal/latitudinal dependence.

Recently, an analysis by Strickland et al. (2004) of ultraviolet airglow measurements by the GUVI instrument concluded that the HFG solar model adequately characterized soft X-ray fluxes, as did the NRLEUV model. This conclusion is dependent on airglow emission cross-sections as well as instrument calibration. If it is correct, then either the SEE measurements of H Lyman-β are too low, or there is something seriously amiss in the established ion chemistry, or we are missing a source of E-region ionization altogether. Furthermore, it is impossible to explain the AE photoelectron fluxes without an increase in the HFG soft X-rays (e.g., Richards and Torr, 1984; Strickland et al., 1999; Solomon et al., 2001). These, measurements, too, could be wrong, or all of these models could be using erroneous cross-sections. An alternative possibility is that solar X-rays shortward of ~5 nm, which are inefficient exciters of ultraviolet airglow due to their penetration depth, are more intense than previously suspected. As solar minimum approaches, TIMED and SORCE in combination with multiple calibration rockets will obtain a full description of the solar spectrum and its variation, which may finally resolve these issues.

Acknowledgements

This research was supported by NASA grants NAG5-5335 and NAG5-11410 to the National Center for Atmospheric Research. NCAR is supported by the National Science Foundation.

References

Bailey, S.M., Woods, T.N., Canfield, L.R., Korde, R., Barth, C.A., Solomon, S.C., Rottman, G.J. Sounding rocket measurements of the solar soft X-ray irradiance. Sol. Phys. 186, 243, 1999.

Bailey, S.M., Woods, T.N., Barth, C.A., Solomon, S.C., Canfield, L.R., Korde, R. Measurements of the solar soft X-ray irradiance from the Student Nitric Oxide Explorer: first analysis and underflight calibrations. J. Geophys. Res 105, 27179, 2000.

Bailey, S.M., Barth, C.A., Solomon, S.C. A model of nitric oxide in the lower thermosphere. J. Geophys. Res. 107, 1205, doi:10.1029/2001JA000258, 2002.

Bilitza, D. International Reference Ionosphere 2000. Radio Sci. 36, 261, 2001.

Buonsanto, M.J., Solomon, S.C., Tobiska, W.K. Comparison of measured and modeled solar EUV flux and its effect on the E-F1 region of the ionosphere. J. Geophys. Res. 97, 10513, 1992.

Buonsanto, M.J., Richards, P.G., Tobiska, W.K., Solomon, S.C., Tung, Y.-K., Fennelly, J.A. Ionospheric electron densities calculated using different EUV flux models and cross sections: comparison with radar data. J. Geophys. Res. 100, 14569, 1995.

Doe, R.A., Thayer, J.P., Solomon, S.C. Solar control of ionospheric plasma density: implications for solar spectral shape and variance, J. Geophys. Res., 2005, in press.

Feng, W., Ogawa, H.S., Judge, D.L. The absolute solar soft X-ray flux in the 20–100 Å region. J. Geophys. Res. 94, 9125, 1989.

Friedrich, M., Torkar, K.M. FIRI: a semiempirical model of the lower ionosphere. J. Geophys. Res. 106, 21409, 2001.

Hedin, A.E. MSIS-86 thermospheric model. J. Geophys. Res. 92, 4649, 1987.

Hinteregger, H.E., Fukui, K., Gilson, B.R. Observational, reference, and model data on solar EUV, from measurements on AE–E. Geophys. Res. Lett. 8, 1147, 1981.

Kazil, J., Kopp, E., Chabrillat, S., Bishop, J. The University of Bern atmospheric ion model: time-dependent modeling of the ions in the mesosphere and lower thermosphere. J. Geophys. Res. 108, 4432, doi:10.1029/2002JD003024, 2003.

Kouris, S.S., Muggleton, L.M. Diurnal variation in *E*-layer ionization. J. Atmos. Terr. Phys. 35, 133, 1973a.

Kouris, S.S., Muggleton, L.M. World morphology of Appleton *E*-layer seasonal anomaly. J. Atmos. Terr. Phys. 35, 141, 1973b.

Marsh, D.R., Solomon, S.C., Reynolds, A.E. Empirical model of nitric oxide in the lower thermosphere. J. Geophys. Res. 109, A07301, doi:10.1029/2003JA010199, 2004.

Ogawa, H.S., Canfield, L.R., McMullin, D., Judge, D.L. Sounding rocket measurement of the absolute solar EUV flux utilizing a silicon photodiode. J. Geophys. Res. 95, 4291, 1990.

Richards, P.G., Torr, D.G. An investigation of the consistency of the ionospheric measurements of the photoelectron flux and solar EUV flux. J. Geophys. Res. 89, 5625, 1984.

Richards, P.G., Fennelly, J.A., Torr, D.G. EUVAC: a solar EUV flux model for aeronomic calculations. J. Geophys. Res. 99, 8981–8992, 1994.

Solomon, S.C. Optical aeronomy. U.S. Natl. Rep. Int. Union Geod. Geophys. 1987–1990, Rev. Geophys. 29, 1089, 1991.

Solomon, S.C., Hays, P.B., Abreu, V.J. The auroral 6300 Å emission: observations and modeling. J. Geophys. Res. 93, 9867, 1988.

Solomon, S.C., Abreu, V.J. The 630 nm dayglow. J. Geophys. Res. 94, 6817, 1989.

Solomon, S.C., Bailey, S.M., Woods, T.N. Effect of solar soft X-rays on the lower ionosphere. Geophys. Res. Lett. 28, 2149, 2001.

Strickland, D.J., Bishop, J., Evans, J.S., Majeed, T., Shen, P.M., Cox, R.J., Link, R., Huffman, R.E. Atmospheric ultraviolet radiance integrated code (AURIC): theory, software, inputs, and selected results. J. Quant. Spect. Rad. Trans. 62, 689, 1999.

Strickland, D.J., Lean, J.L., Meier, R.R., Christensen, A.B., Paxton, L.J., Morrison, D., Craven, J.D., Walterscheid, R.L., Judge, D.L., McMullin, D.R. Solar EUV irradiance variability derived from terrestrial far ultraviolet dayglow observations. Geophys. Res. Lett. 31, L03801, doi:10.1029/2003GL018415, 2004.

Titheridge, J.E. Model results for the ionospheric E region: solar and seasonal changes. Ann. Geophys. 15, 63, 1997.

Titheridge, J.E. Modelling the peak of the ionospheric E-layer. J. Atmos. Sol. Terr. Phys. 62, 93, 2000.

Titheridge, J.E. Model results for the daytime ionospheric E and valley regions. J. Atmos. Sol. Terr. Phys. 65, 129, 2003.

Tobiska, W.K., Woods, T.N., Eparvier, F.G., Viereck, R., Floyd, L., Bouwer, D., Rottman, G.J., White, O.R. The SOLAR2000 empirical solar irradiance model and forecast tool. J. Atmos. Sol. Terr. Phys. 62, 1233, 2000.

Trost, T.F. Electron concentrations in the *E* and upper *D* region at Arecibo. J. Geophys. Res. 84, 2736, 1979.

Warren, H.P., Mariska, J.T., Lean, J. A new reference spectrum for the EUV irradiance of the quiet Sun: 1. Emission measure formulation. J. Geophys. Res. 103, 12077, 1998.

Woods, T., Rottman, G., Harder, J., Lawrence, G., McClintock, B., Kopp, G., Pankratz, C. Overview of the EOS SORCE mission. SPIE Proc. 4135, 192, 2000.

Woods, T.N., Eparvier, F.G., Bailey, S.M., Chamberlain, P.C., Lean, J., Rottman, G.J., Solomon, S.C., Tobiska, W.K., Woodraska, D. The solar EUV experiment SEE: mission overview and first results. J. Geophys. Res. 110, A01312, doi:10.1029/2004JA010765, 2005.